PHOTOMASK

BACUS—The international technical group of SPIE dedicated to the advancement of photomask technology.

2nd Place Best Paper - PM14

Characterization of a New Polarity Switching Negative Tone E-beam Resist for 14 nm and 10 nm Logic Node Mask Fabrication and Beyond

T. Faure, A. Zweber, S. Nash, J. Malenfant, and R. Bowley, IBM Corporation, 1000 River Street, Essex Junction, VT, USA 05452

L. Bozano, M. Sanchez, R. Sooriyakumaran, and L. Sundberg, IBM Corporation, 650 Harry Road, San Jose, CA, USA 95120

Y. Sakamoto, M. Kagawa, and T. Isogawa, Toppan Photomasks, Inc., 1000 River Street, Essex Junction, VT, USA 05452

T. Senna, M. Tanabe, T. Komizo, and I. Yoshida, Toppan Printing Co., Ltd., 7-21-33 Nobidome, Niiza, Saitama, 352-8562, Japan

K. Masunaga, S. Watanabe, and Y. Kawai, ShinEtsu Chemical Co. Ltd, 28-1, Nishifukushima, Kubiki-ku, Joetsu-shi, Niigata, Japan

ABSTRACT

The critical layer masks for 14 nm and 10 nm logic nodes are typically bright field, and the key features are opaque structures on the mask. In order to meet the tight critical dimension (CD) requirements on these opaque features the use of a high quality negative tone chemically amplified e-beam resist (NCAR) is required. Until very recently the only negative tone e-beam resists available for use by the mask industry were the traditional cross linking type in which ebeam exposure cross links the material and makes it insoluble in developer. In this paper we will describe the performance of a new polarity switching type of NCAR resist that works by changing the solubility of the exposed resist without cross linking. This has the advantage of significantly

Table 1. Material matrix. Comparison of the evaluated resists: crosslink (XL) vs polarity switch (PS) and its chemical modifications.

Resist	Sensitivity (# passes)	Chemistry X-link (XL)/Polarity Switch (PS)	Polymer	PAG
A1	2	XL	I	1
B1	2	PS	III	3
A2	4	XL	I	1
B2	4	PS	III	3
A3	8	XL	I	1
C	2	PS	II	2

BACUS NEWS

MARCH 2015
VOLUME 31, ISSUE 3

TAKE A LOOK INSIDE:

INDUSTRY BRIEFS
—see page 16

CALENDAR
For a list of meetings
—see page 17

SPIE.

9235-24

EDITORIAL

Rich Larson, an original Maskmaker

By **John Whittey** and **Greg Easley**



Richard Ole Larson, 68 of Manteca passed away Monday, January 19th at his residence due to complications resulting from his fight with cancer. He is survived by his wife Sandra Larson and his three children Tristel, Brandon and Garrett.

Rich was the recipient of the 2012 SPIE BACUS Lifetime Achievement Award for his exemplary service to the photomask making community. Fresh off his third tour of duty as a US Navy Aviator he began his career at MicroMask in 1973 working for Ron Tredway, Bob Whiteside and Joe Ross. Even though Rich was an English Literature major, operations management was his forté. Rich's career path took him on to Ultratech Photomask, Photronics, and DuPont/Toppan where he successfully led Operations to record breaking performances at each company. Rich liked to simplify challenging tasks, claiming it was the way he was taught to do things back on the farm in Minnesota, one thing at a time.

Mr. Larson was running operations back in the early 1980's at Ultratech Photomask when they became the first photomask manufacturer to ship $1,000,000 worth of production in a single month, a milestone at the time. He also led DuPont/Toppan to exceed 100 direct write photomasks shipped per day in his last photomask tour of duty. Rich retired from Toppan as the Santa Clara site manager in 2008.

Probably the best description of Rich and his career was that he was an original Maskmaker. Helping to develop processes and systems currently deployed across the industry. It is hard to imagine how many sets of masks Rich was responsible for manufacturing and shipping in 35 years. He accomplished this by leading by example, inspiring tremendous loyalty and admiration among his subordinates. Rich was a mentor to many of our industry's current and former managers in his various positions. It is hard to put into a few words Rich's best traits, but integrity, loyalty, honesty, perseverance, hardworking, and attention to details of all kinds (work and family), are just a few of them. He will be sorely missed!!

An obituary with more about Rich Larson is at **http://goo.gl/KkOCAe**

BACUS

N • E • W • S

BACUS News is published monthly by SPIE for BACUS, the international technical group of SPIE dedicated to the advancement of photomask technology.

Managing Editor/Graphics Linda DeLano

Advertising Lara Miles

BACUS Technical Group Manager Pat Wight

■ **2015 BACUS Steering Committee** ■

President
Paul W. Ackmann, *GLOBALFOUNDRIES Inc.*

Vice-President
Jim N. Wiley, *ASML US, Inc.*

Secretary
Larry S. Zurbrick, *Keysight Technologies, Inc.*

Newsletter Editor
Artur Balasinski, *Cypress Semiconductor Corp.*

2015 Annual Photomask Conference Chairs
Naoya Hayashi, *Dai Nippon Printing Co., Ltd.*
Bryan S. Kasprowicz, *Photronics, Inc.*

International Chair
Uwe F. W. Behringer, *UBC Microelectronics*

Education Chair
Artur Balasinski, *Cypress Semiconductor Corp.*

Members at Large
Frank E. Abboud, *Intel Corp.*
Paul C. Allen, *Toppan Photomasks, Inc.*
Michael D. Archuletta, *RAVE LLC*
Peter D. Buck, *Mentor Graphics Corp.*
Brian Cha, *Samsung*
Thomas B. Faure, *IBM Corp.*
Brian J. Grenon, *Grenon Consulting*
Jon Haines, *Micron Technology Inc.*
Mark T. Jee, *HOYA Corp, USA*
Patrick M. Martin, *Applied Materials, Inc.*
M. Warren Montgomery, SUNY, *The College of Nanoscale Science and Engineering*
Wilbert Odisho, *KLA-Tencor Corp.*
Jan Hendrik Peters, *Carl Zeiss SMS GmbH*
Michael T. Postek, *National Institute of Standards and Technology*
Abbas Rastegar, *SEMATECH North*
Emmanuel Rausa, *CYMER LLC.*
Douglas J. Resnick, *Canon Nanotechnologies, Inc.*
Thomas Struck, *Infineon Technologies AG*
Bala Thumma, *Synopsys, Inc.*
Jacek K. Tyminski, *Nikon Research Corp. of America (NRCA)*
Michael Watt, *Shin-Etsu MicroSi, Inc.*

SPIE.

P.O. Box 10, Bellingham, WA 98227-0010 USA
Tel: +1 360 676 3290
Fax: +1 360 647 1445
www.SPIE.org
help@spie.org

©2015

All rights reserved.

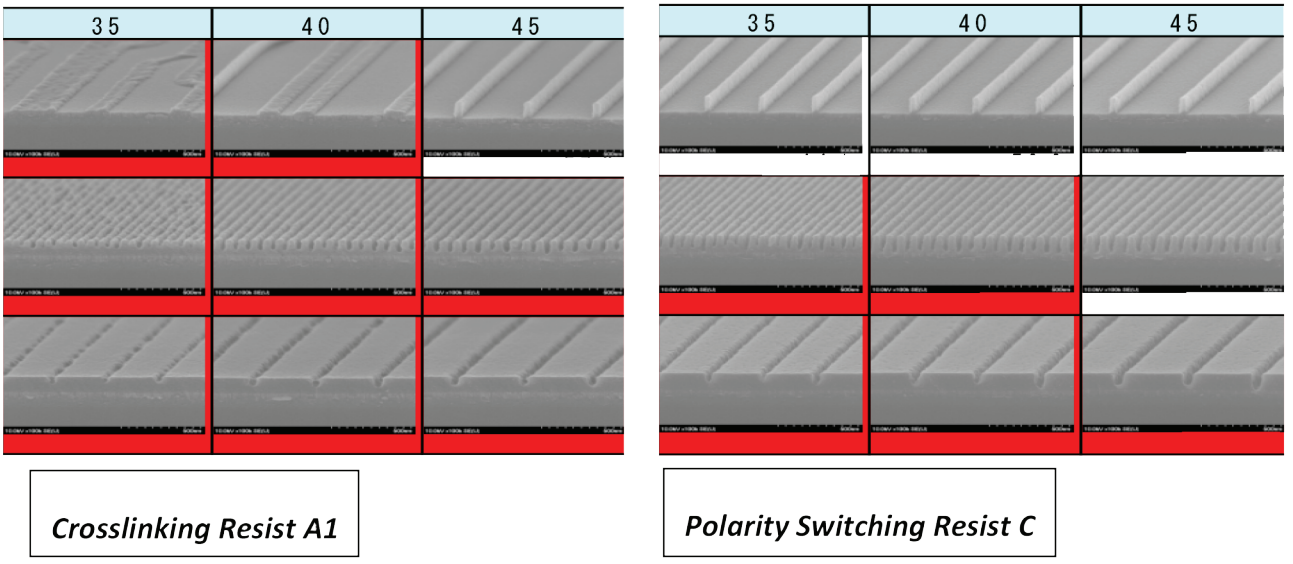


Figure 1. SEM comparison of minimum feature size performance of traditional cross linking NCAR resist A1 versus polarity switching NCAR resist C. All SEM images are of developed resist images.

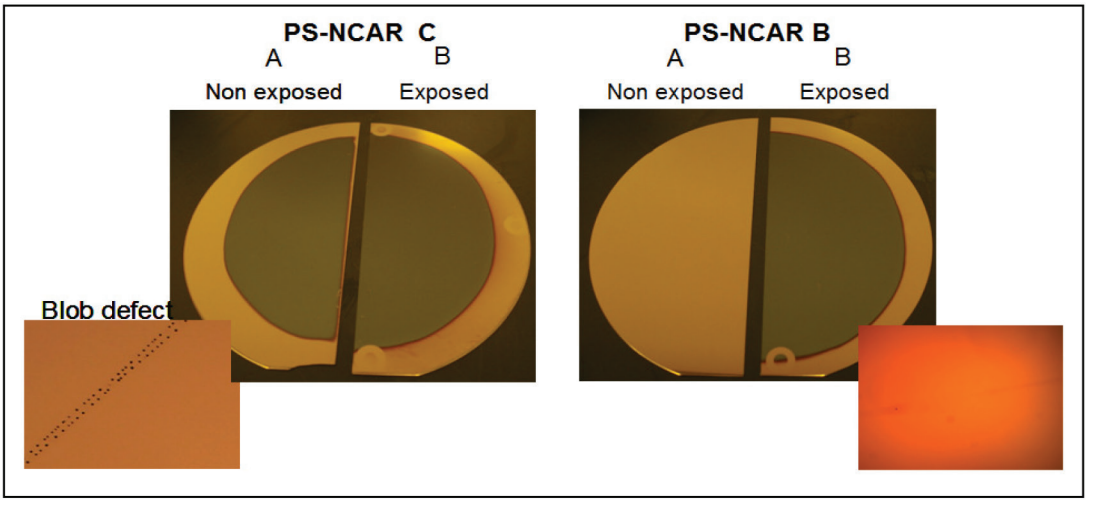


Figure 2. a). Example of blob defects residual resist found in unexposed developed areas seen with original formulation polarity switching resist C. b). Confirmation of no blob defects and no residual resist seen in unexposed developed areas for re-formulated polarity switching resist B.

reduced swelling and scumming and resulted in major improvements in the resolution of heavily nested features and small clear features on the mask. Additional detailed characterization results will be described.

1. Introduction

Negative-tone resists are required for bright field masks to retain low e-beam write times. Conventional crosslinking negative-tone chemically amplified resists (NCAR), though, often suffer from micro-bridging, swelling and higher line edge roughness (LER) than positive-tone chemically amplified resists (PCAR). We previously presented our results using an alternative approach for a negative-tone resist via polarity switching.[1] Polarity switching is the mechanism used for PCAR development. By implementing this in a negative-tone image, we hoped to remove the common drawbacks of conventional crosslinking negative-tone resists.

The initial polarity switching resist had higher resolution than the process of record crosslinking resist but, unfortunately, a high number of defects (previously named “blobs”). We discovered that the acid generated from the photoacid generator (PAG) was outgassing which caused the unexposed areas to become partially

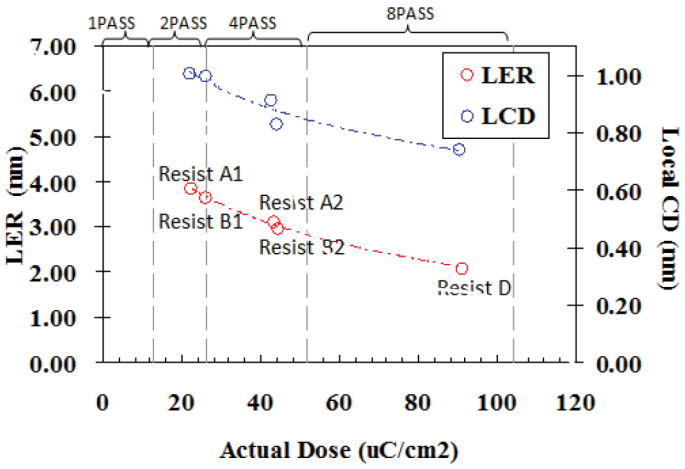


Figure 3. Line Edge Roughness (LER) and Local CD uniformity performance for different NCAR resists. Dose values are for nested line/space structures.

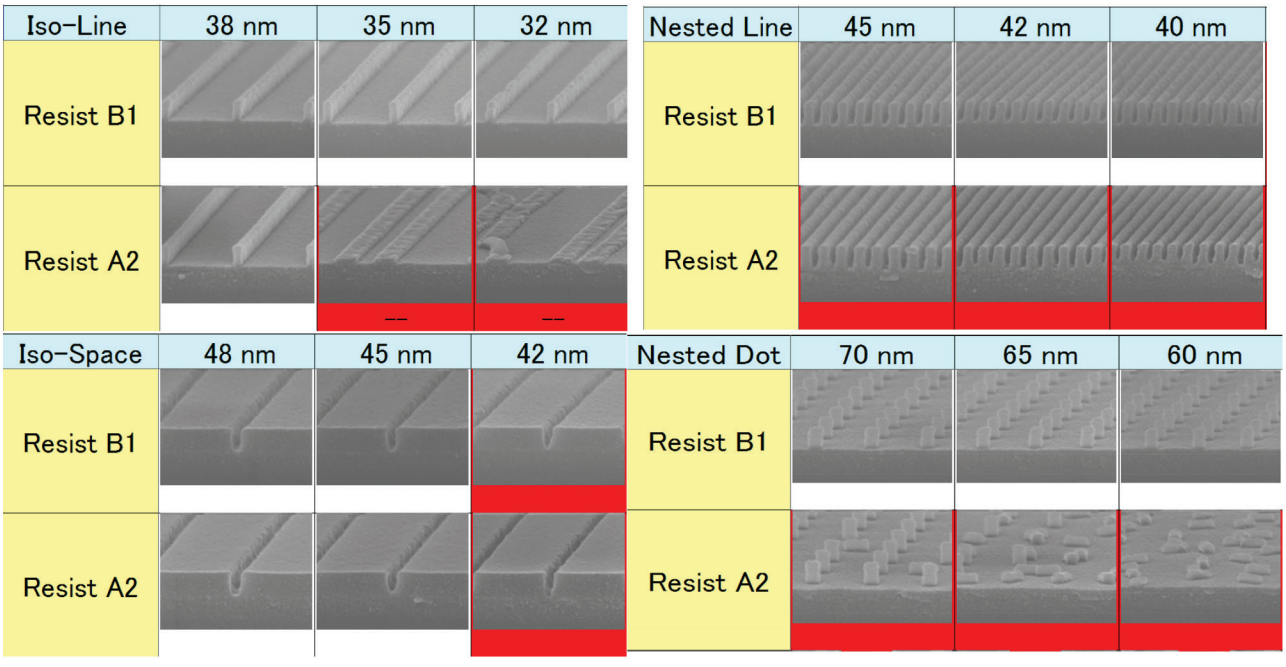


Figure 4. Resist cross-section SEM images of crosslinking resist A2 and polarity switching resist B1. Resist thickness is 125 nm on a PSM substrate.

insoluble in the developer solution. The result was redeposition of the resist onto the developed area which subsequently blocked etch and left a defective area on the mask. Making changes to both the polymer structure and the PAG yielded a high resolution negative-tone resist without the "blob" defects. This paper will compare this new polarity switching negative-tone resist with conventional crosslinking e-beam NCAR resists.

2. Experimental

2.1 Materials

The polarity switching resist is the first of its kind to be evaluated as not only an e-beam resist but also for mask making. It was apparent early on that it had the potential to surpass current e-beam resists in many performance areas. Table 1 illustrates the matrix of resists that were assessed in this paper. Resist C in table 1 represents the original formulation of the polarity switching resist. Figure 1 gives an example of the improved minimum feature size performance that was observed with resist C versus traditional cross linking

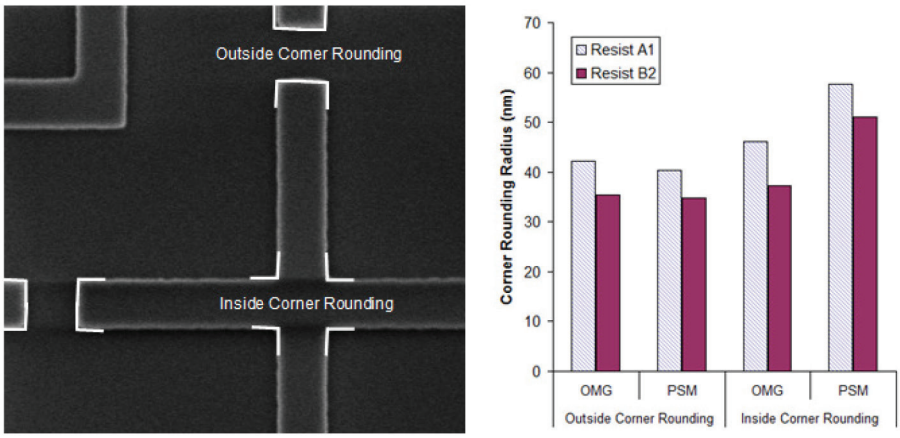


Figure 5. Mask corner rounding radius plotted with various changes in resist sensitivity and blank type at 200 nm feature size.

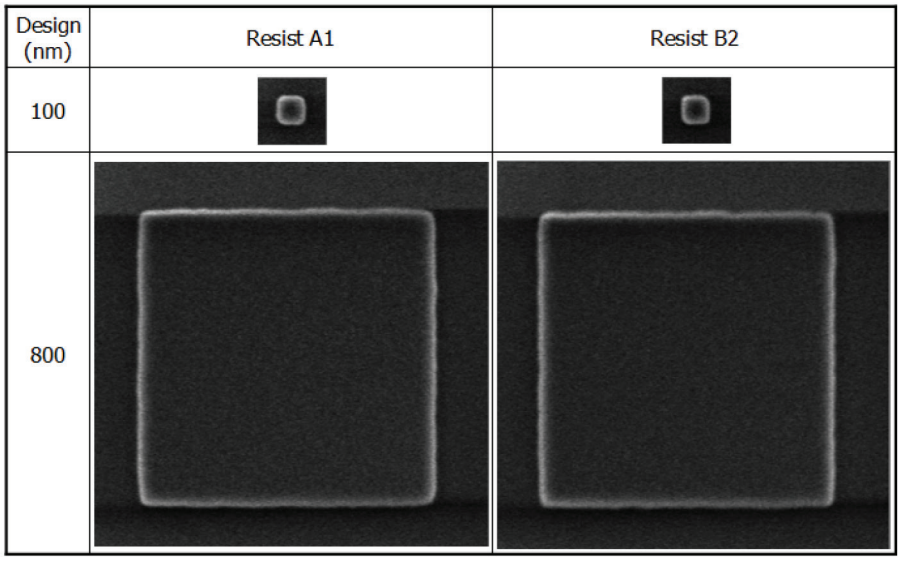


Figure 6. Mask SEMs for 800 and 100 nm square features.

resist A1. As mentioned above, resist C had a high number of blob defects as shown in figure 2a. After much experimentation it was discovered that the blobs were caused by outgassing of the acid generated from the photoacid generator (PAG) which caused the unexposed areas to become insoluble and resulted in the re-deposition of resist onto the developed area. This understanding led to development of improved polarity switching resist materials B1 and B2 (see table 1) which had changes to both the polymer and PAG and showed no evidence of blob defects as shown in figure 2b. The remainder of this paper focuses on comparing the performance of the improved polarity switching resists B1 and B2 versus crosslinking resists A1 and A2 listed in table 1.

3. Resist Sensitivity Considerations

One of the biggest challenges for 14 nm and 10 nm optical masks is to meet tight critical dimension uniformity (CDU) requirements. As shown in figure 3 and also by other authors[2,3,4] the line edge roughness (LER) and local CDU measured over a 500 um x 500 um area strongly depends on exposure dose applied to each resist system. By assessing the resist sensitivity impact on local CDU for the new resist system, the proper sensitivity can be selected that will meet 14 nm and 10 nm CDU requirements. As the figure indicates, the local CD uniformity and line edge roughness both improve with increasing dose due to a reduction in the e-beam shot noise, an increase in the number of exposure passes (averages errors), and by a reduction of chemical diffusion effects in the resist. The drawback to using lower sensitivity resists is that the higher exposure doses require 4 to 8 exposure passes on a typical 50keV e-beam writer which leads to a large increase in mask write times and low e-beam tool throughput. Based on these results and given the tight CDU mask specifications for 14 nm and 10 nm masks, the decision was made to pursue implementation of

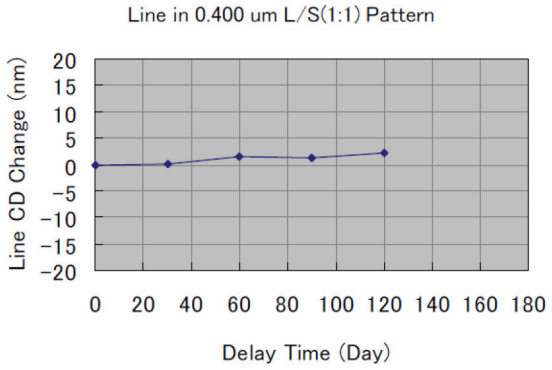


Figure 7. Post coat delay of Resist B1.

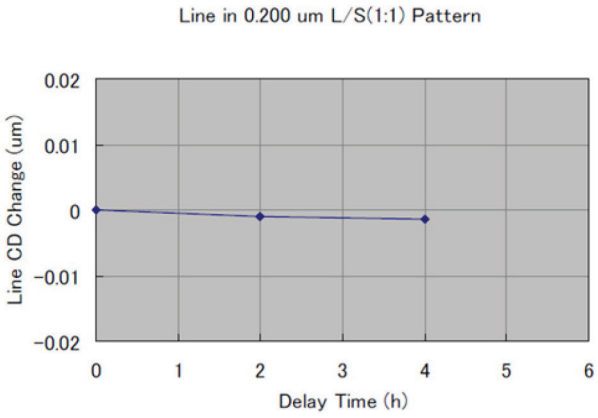


Figure 9. Post exposure delay in air for Resist B2.

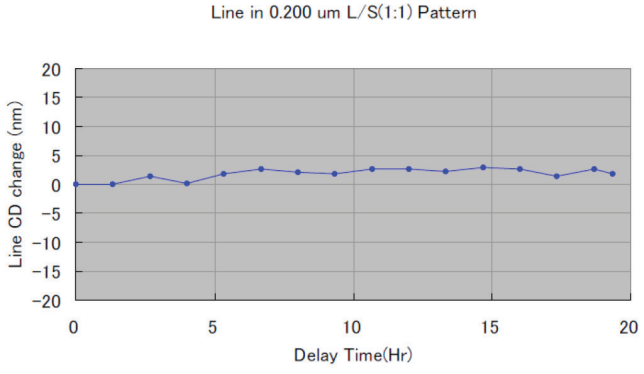


Figure 8. Post exposure delay in vacuum for Resist B2.

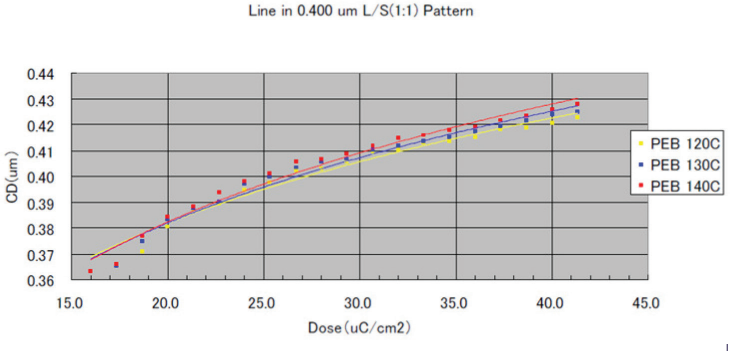


Figure10. Dose and post exposure bake latitude for Resist B1.

the lower sensitivity 4 pass version of the polarity switching resist B2 which was a reasonable tradeoff between lower e-beam tool throughput and better local CD variation.

4. Evaluation of Basic Properties of Polarity Switching Resist

4.1 Minimum Feature Size

A first look at resolution performance was obtained by taking resist cross section SEM images. The images provide a glimpse at the resist profile quality and image resolution for isolated line, nested line, isolated space, and dot feature types. In Figure 4, new Resist B1 and traditional crosslinking Resist A2 feature profiles are compared at 125 nm resist thickness on an attenuated PSM blank. The isolated line and dot features of Resist A2 are slightly larger near the top and tend to collapse and delaminate, while Resist B1 remains intact for at least an additional 10 nm. The nested Resist A2 and Resist B1 features both have some footing although Resist A2 is more significantly underprocessed, where the spaces are not resolving to the same degree as Resist B1. Lastly, Resist A2 isolated spaces have some t-topping, but the amount of footing and resolution is similar between the two resists. In general, new Resist B1 has superior overall resolution performance over traditional crosslinking Resist A2 for which the features have some t-topping and delaminate from the surface more readily.

4.2 Mask Corner Rounding

Mask corner rounding radius was measured for differing resist sensitivity and blank types to demonstrate example mask performance and trends. Corner rounding measurements were taken using an industry standard metrology tool using 200 nm feature outside and inside corners as depicted in Figure 5. The measurement includes establishing the region of interest around the corner, finding the bisecting line through the corner, and geometrically calculating the corner rounding radius as described in more detail previously.[5] As shown in Figure 5, lower sensitivity Resist B2 has improved corner rounding performance over high sensitivity Resist A1. As described in Section 2, lower sensitivity resist usage reduces e-beam shot noise, increases averaging with multiple exposure passes, and reduces resist chemical diffusion effects for an overall pattern fidelity improvement. Corner rounding improvement of an average of 7 nm was observed for inside and outside corners for both OMOG and attenuated PSM masks. It can be noted that the attenuated PSM inside corner rounding performance is worse than OMOG , which is most likely due to local etch loading effects and the longer etch process required for removing the thicker chrome hard mask and thicker attenuated PSM absorber. In Figure 6, SEM images of representative dot features with Resists A1 and B2 are shown for 100 and 800 nm design sizes. The corner rounding improvements are subtle in the SEM images but consistently measurable.

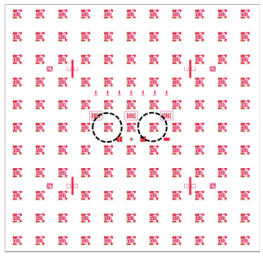


Figure 11. Dry Etch Test Patterns: CD uniformity and linearity test mask.

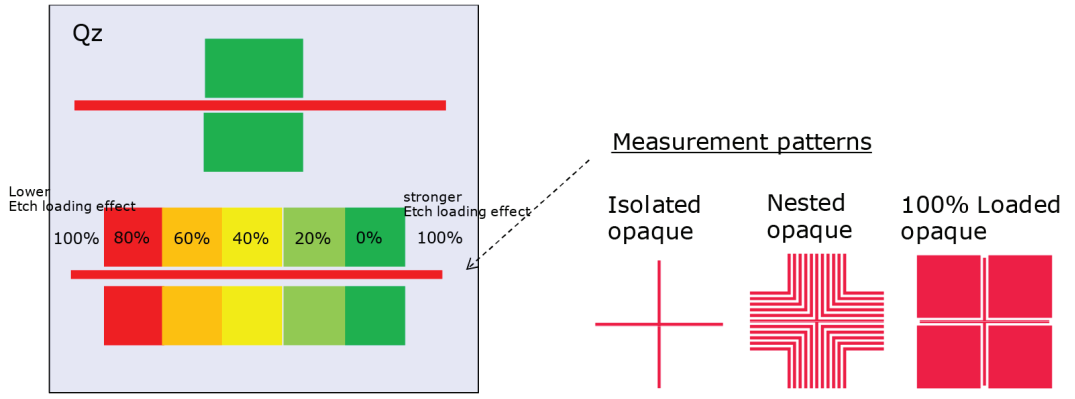


Figure 12. Dry Etch Test Patterns: Global etch loading test pattern.

4.3 Resist Stability

With control of image size moving to +/- 2nm and tighter,[6] resist stability is critical. Resist stability post coat, post exposure in vacuum, and post exposure in air were measured for polarity switching resists B1 and B2. Figure 7 shows resist B1 stability with delay post coat prior to writing, and the influence is less than 2 nm over 60 days. Figure 8 is the CD stability of resist B2 with delay post exposure in vacuum which simulates the delay while writing a mask within the e-beam system. The change in critical dimension is less than 3 nm over 20 hours. Figure 9 demonstrates the stability of resist B2 post exposure in air to simulate CD change as the written mask is moved from the write chamber to post exposure bake. The CD change is less than 2nm over 2 hours. This result confirms that controls are needed to execute post exposure bake consistently and immediately after exposure to meet CD requirements as is similar with other chemically amplified resists. In general, the stability of the polarity switching resist is acceptable for manufacturing.

4.4 Process Window

CD control through post exposure bake condition and dose was also evaluated to examine the new resist material process window. Three post exposure bake temperatures were evaluated: 120°, 130°, and 140°C, where the process of record operating temperature is 130°C. As shown in Figure 10, the differences among the three tested temperatures are minimal with less than 0.2 nm per degree Celsius. At any of the three temperatures, the dose latitude is manageable at 0.5 nm/% dose.

5. Dry Etching Properties

The dry etch characteristics of COG, PSM and OMOG films were compared using the different NCAR resists. The test pattern used for critical dimension (CD) uniformity and CD linearity studies is shown in Figure 11. The test pattern has a 1% e-beam written pattern density (i.e. 99% of surface area of the mask ends up being etched). Across mask CD is measured using an 11 x 11 array of measurement structures covering a 132 x 132-mm2 area. Figure 12 shows the test mask design used to evaluate the dry etch global loading effect evaluation. One hundred CD measurement sites are placed across the different loading areas of the mask. Isolated opaque, nested opaque and isolated clear features were used for this global etch loading test. All test masks were printed using a 50 keV e-beam writer and were baked and developed using standard tools and processes common to the industry. All chrome films were etched in an inductively coupled plasma (ICP) etcher with chlorine-based chemistry. Next, the ebeam resist was stripped and the MoSi films were etched in an ICP etcher with fluorinated chemistry. The chrome hard mask was removed from the samples using industry-standard wet etching for expediency and to avoid introducing another source of variability.

5.1 Dry etch durability

The dry etch durability of resist B2 was calculated using the resist thickness post develop and the resist thickness post Cr etch. The resist thickness was measured by ellipsometry. Two kinds of etch recipes were studied: an OMOG etch recipe and an attenuated PSM etch recipe. A comparison of the resist etching rates of resist A1 and B2 for both the OMOG recipe and attenuated PSM recipe is shown in Figure 13. As indicated in the figure the dry etch durability of resist B2 with the OMOG recipe is 7% better than resist A1, and the dry etch durability of resist B2 with the attenuated. PSM recipe is 18% better than resist A1. The improved dry etch durability of the polarity switching resist B2 is expected based on the fact that it has a lower Ohnishi number[7] than cross linking resist A1. The lower Ohnishi number for resist B2 means that there is more carbon and less oxygen in the polymer versus resist A1, and this has been shown to correlate directly to improved dry etch resistance. In the case of the polarity switching resist B2, the polar OH group is reduced after e-beam exposure and post expose bake which makes the resist switch to negative tone and simultaneously achieve a lower Ohnishi number than the conventional cross linking resist A1. The better dry etch resistance for polarity switching resist B2 enables the use of a thinner resist than resist A1 which is helpful for improving the resolution of small features on the mask. For etching PSM masks it was found that resist B2 could be 250 angstroms thinner than resist A1.

5.2 CD Linearity

The two circled regions on figure 11 indicate the locations where the linearity measurements were taken on the mask. At each of the two locations X and Y measurements of linearity were taken, and a total of four CD data were averaged to generate the data used on the linearity curves shown in figure 14 below. Figure 14 compares the dry etch contribution to CD linearity for resists A1 and B2 for attenuated PSM masks. A comparison of the etch contribution range for attenuated PSM is shown in Figure 15.

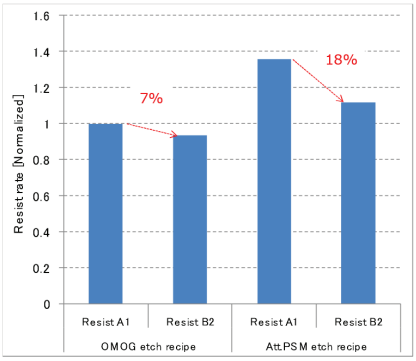


Figure 13. Dry etch durability.

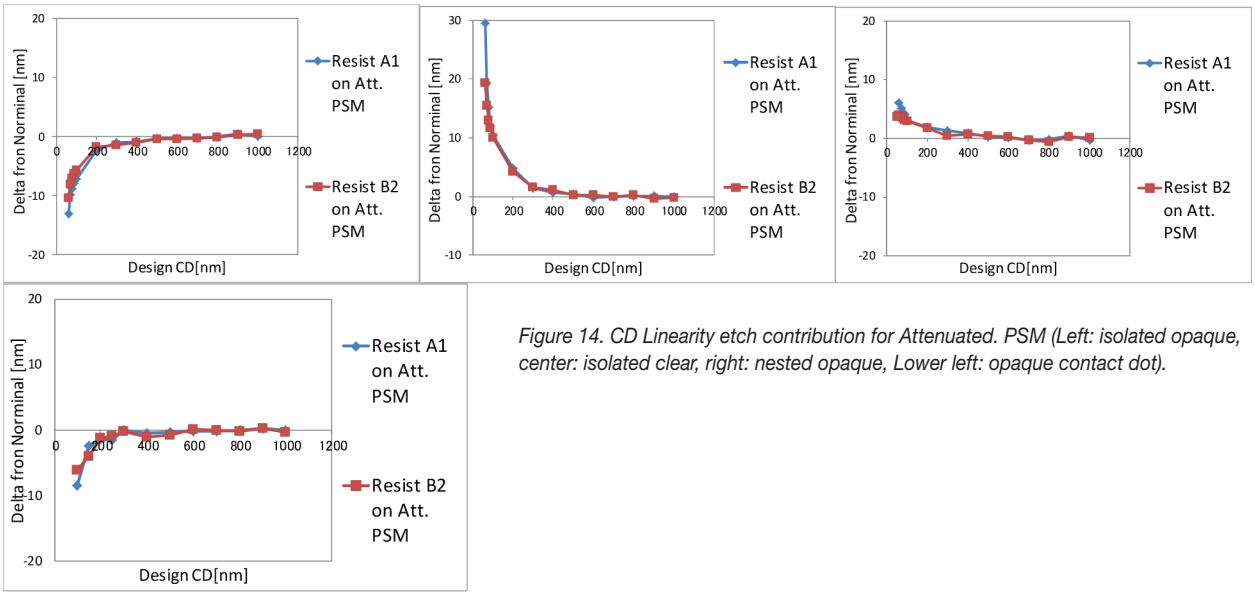


Figure 14. CD Linearity etch contribution for Attenuated. PSM (Left: isolated opaque, center: isolated clear, right: nested opaque, Lower left: opaque contact dot).

The feature size range studied was 60 nm to 1000 nm for isolated opaque, isolated clear and nested opaque structures. For opaque contact dot structures, the feature size range studied was 100 nm to 1000 nm. The data for attenuated PSM indicates that the etch CD linearity performance of polarity switching resist B2 is clearly better than cross linking resist A1. This is most likely due to the higher dry etch resistance of resist B2 which enabled use of a 250 angstrom thinner resist thickness than resist A1 and helped reduce resist consumption due to faceting of resist during the etch on the smallest isolated opaque line and contact dot features. A comparison of the CD linearity range in final MoSi for both OMOG and attenuated PSM masks is shown in Figure 16. The data for both OMOG and attenuated PSM indicates that the CD linearity performance of resist B2 is better than resist A1 and A2.

The improved final MoSi linearity performance of polarity switch resist B2 is due to the improved resolution of smaller feature sizes, less swelling and scumming in clear features, and improved dry etch resistance.

5.3 CD Uniformity and Etch Bias of Dry Etch

The etch contribution to across mask global CD uniformity performance was calculated using a point-by-point subtraction of final CD data and resist CD data for a 200 nm isolated feature. Figures 17 and 18 show the etch CD uniformity in bubble plot form for OMOG and attenuated PSM respectively. Figure 17 indicates the etch contribution to global CD performance of resist B2 is better than other resists. Figure 18 shows the etch contribution to global CD performance of resist B2 is similar with resist A1. A comparison of the etch bias performance of the different resists for OMOG and PSM masks is shown in Figure 19. By definition etch bias means the subtraction between resist CD and final MoSi CD. These etch bias values came from the average of 121 measurements of 200 nm isolated opaque features across the mask. In general there were only small differences (2-3 nm) in etch bias measured for masks processed using the different NCAR resists with resist B2 tending to have slightly lower etch bias versus resist A1 and A2.

5.4 Global Etch loading effect

An assessment of the global etch loading effect for resist A1 and resist B2 was conducted by measuring the etch bias of 300nm isolated opaque features and 300nm nested opaque features across the 100% to 0% loading test pattern shown in the bottom half of figure 12. Generally, attenuated PSM masks have a stronger etch loading effect due to the use of a much thicker Cr hard mask film

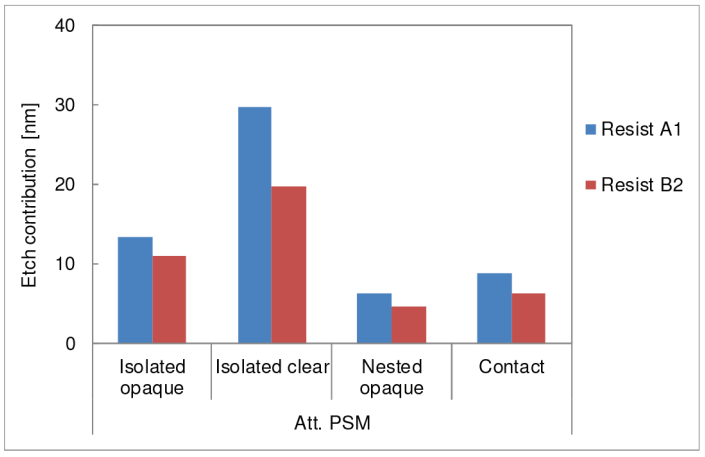


Figure 15. The etch contribution range comparison: Att. PSM.

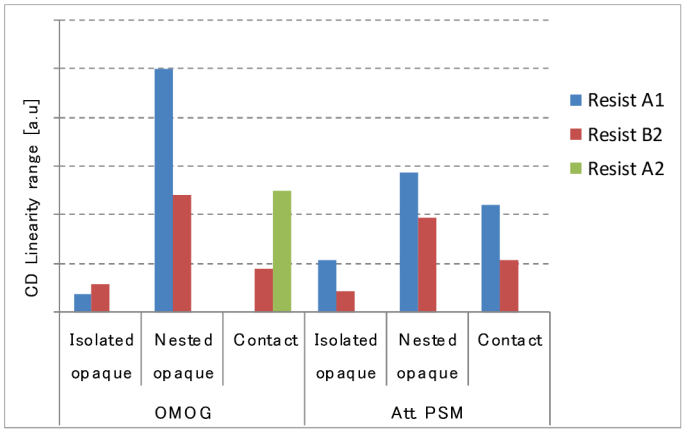


Figure 16. Comparison of the final MoSi CD linearity range for PSM and OMOG masks built with resist A1, A2, and B2..

(45nm -55 nm) compared to OMOG masks which only use a 4-5 nm thick Cr hard mask. Figure 20 compares the global loading performance of the etching components (final MoSi minus resist) for PSM masks built with resist A1 and resist B2. The results in the figure show that the global loading performance of the etching components of resist B2 is significantly better than resist A1. The improved etch loading performance of resist

B2 for PSM masks is most likely due to a combination of having better dry etch durability, thinner resist thickness, and potentially less resist and final MoSi sidewall variation as a function of pattern density versus resist A1.

6. Global CD Uniformity Results

After completing optimization of the ebeam exposure, develop, and dry etch processing conditions for the new 4 pass polarity switching resist B2, a comparison of the final etched MoSi across mask CD uniformity performance was done versus masks built with other traditional cross linking resists for several different 14 nm logic critical layers. As figure 21 below shows, the final mask CD uniformity was better in all cases with resist B2 with the most improvement being achieved on the 14 nm PSM V0 (via) level mask. The improved final mask CD uniformity of resist B2 is due to the better local CD uniformity shown in section 2 as well as the reduced etch loading effect shown in section 4.4 and optimized e-beam corrections for CD errors. Figure 22 shows a more detailed analysis of the across mask CD uniformity performance of the 14 nm V0 PSM mask. As indicated by the figure, the post develop CD uniformity of resist B2 was 1.5 nm (3 sigma), and the final MoSi CD uniformity was also 1.5 nm (3 sigma). In this case the measured structure on the mask was a 296 nm x 304 nm opaque via dot. The CD uniformity was calculated as the 3 sigma of the square root of the area for 194 via dots measured across the mask over a 103 mm x 132 mm area. The final CD uniformity of the V0 mask is further reduced to 1.08 nm (3 sigma) if multi-dot averaging of the CD's of 4 individual dots at each of the 194 measurement locations is performed.

7. Manufacturable Minimum Feature Size Performance

7.1 Experimental

Resolution in this section and in previous work[2] is determined by

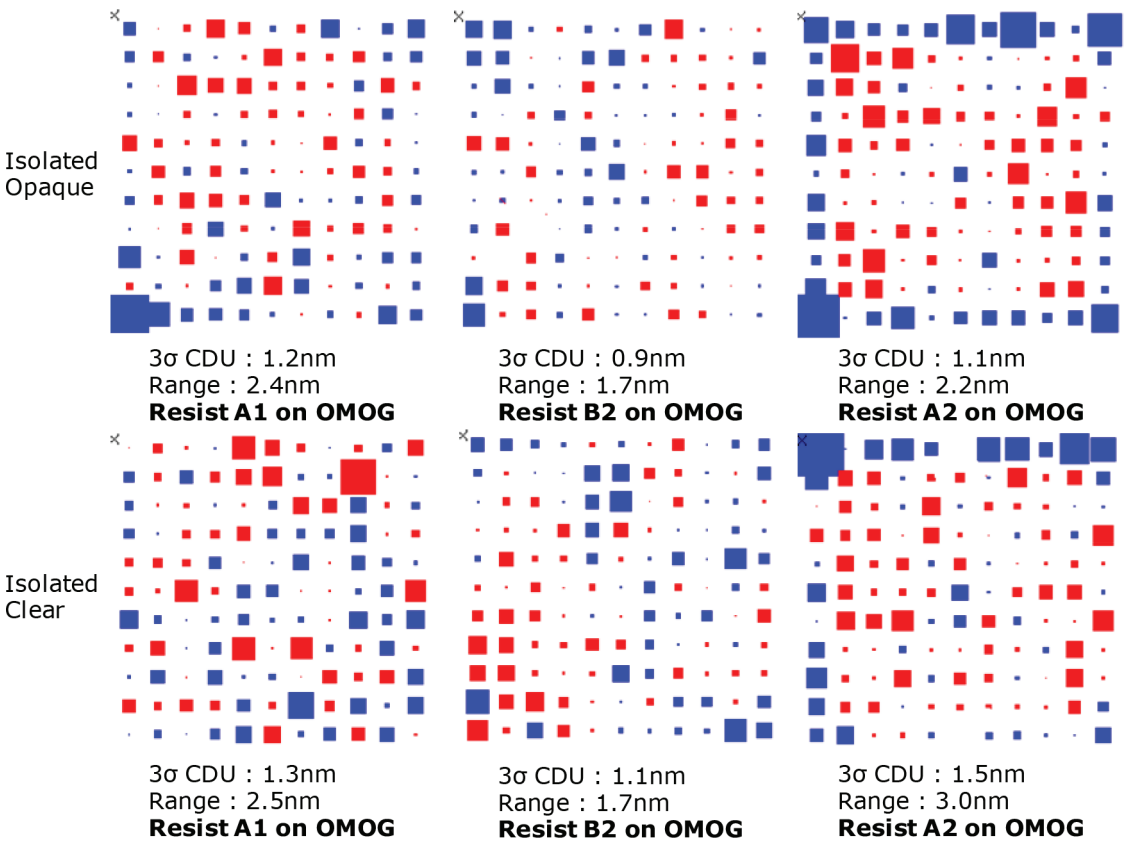


Figure 17. The Etch CD uniformity comparison of resist A1, resist B2 and resist A2 with OMOG.

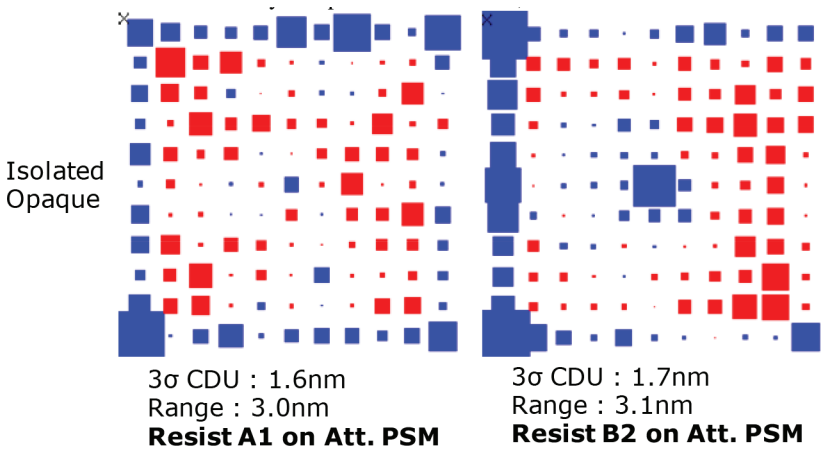


Figure 18. Etch CD uniformity comparison between Resist A1 and Resist B2 with Att.PSM.

the size of sub resolution assist features (SRAFs) in final mask MoSi that pass defect inspection using a 193nm die to database defect inspection system, which we refer to as the manufacturable resolution. The SRAFs vary in length and width systematically as shown in figure 23. For each feature size roughly 1 million SRAFs are inspected, which in Tables 2 and 3 is described by one cell. The tables show results from a manufacturable resolution test with design feature width listed in the column headings and design feature length indicated in the row headings. The cells are color coded to represent the quality of the SRAFs for geometry.

White cells correspond to geometries with no SRAF fails found at inspection, and light solid color (pink) cells represent the onset of assist feature fails transitioning to dark colored (red) cells where the feature size is not manufacturable. Cells listed as N/A

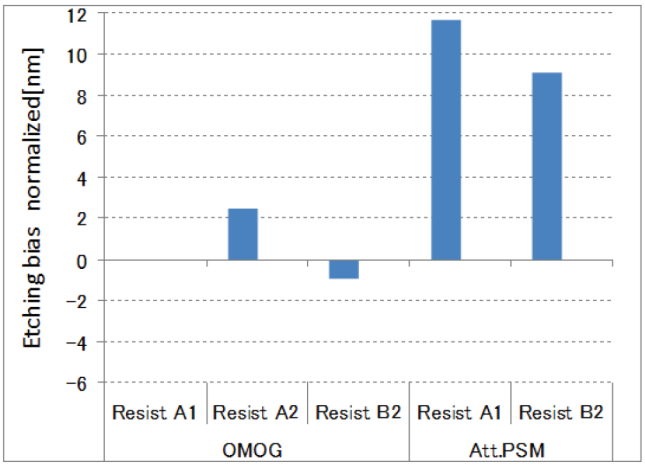


Figure 19. Etch bias (200nm opaque).

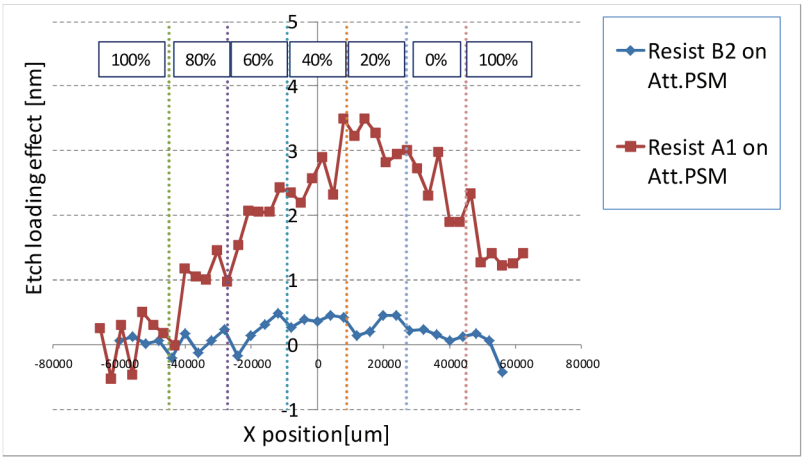


Figure 20. Comparison of etch loading performance of resist A1 and resist B2 for PSM masks. Etch bias of a 300nm opaque feature was measured across different large area pattern densities ranging from 0% to 100% to determine the global loading effect.

were not inspected due to expected high counts of SRAF fails. The definition of an assist feature fail includes missing, broken, or shortened SRAFs. Although resist cross-sections still have a place for resist profile understanding and resist screening, manufacturable resolution provides much more detailed description of the overall resolution performance.

7.2 Minimum feature size performance of OMOG and Attenuated PSM

Tables 2 and 3 compare the manufacturable minimum feature size results for both OMOG and attenuated PSM masks created using several NCAR materials. For OMOG masks, the opaque resolution of resist B2 is the same or slightly worse than resist A1, but the clear resolution of resist B2 is much better than resist A1. The improved clear feature resolution of resist B2 is due to less resist scum and swelling of polarity switching resists relative to traditional crosslinking resists. For attenuated PSM masks, both the opaque and clear resolution of resist B2 is better than resist A1. As Table 3 indicates, the minimum opaque SRAF resolution is improved by 10 nm with a minimum opaque SRAF size of 44 nm being achieved with resist B2 versus a minimum opaque SRAF size of 54 nm with resist A1. In this case the polarity switching resist does a better job of resolving small features in the thicker resist required for use on PSM masks. Another way of analyzing the data in tables 2 and 3 is to plot the total resolution performance of the different NCAR resists as shown in figure 24, which is a valuable way to compare resist materials considering print and process conditions can alter the balance between opaque and clear resolution. In this figure, the y-axis shows the total resolution performance of each resist as the sum of opaque and clear SRAF resolution performance. As the figure indicates, resist B2 clearly gives the best total resolution performance for both OMOG and attenuated PSM masks.

Figure 25 shows examples of SEM top view images of small clear and opaque SRAF features in final MoSi for the different resist systems achieved on OMOG test masks. Design CD sizes

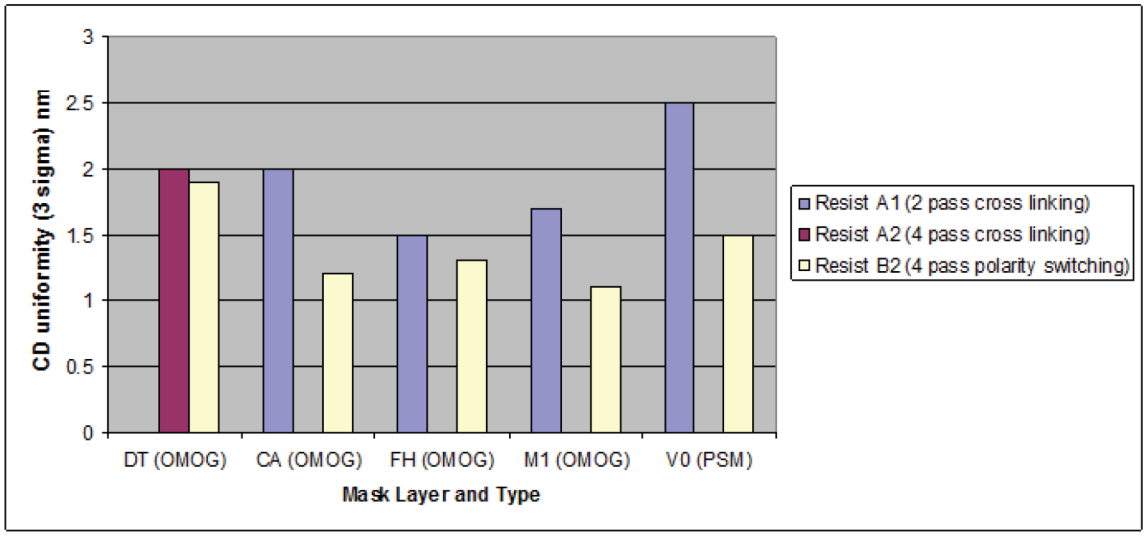
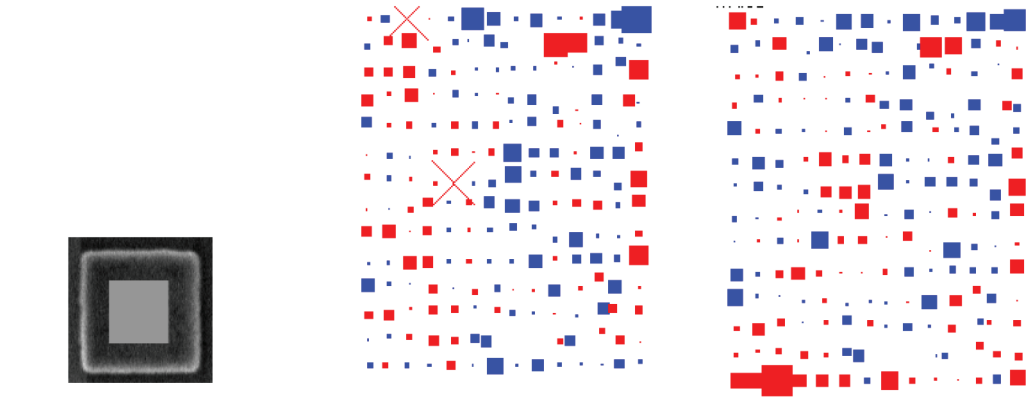


Figure 21. Comparison of across mask global CD uniformity of different NCAR resists using 14 nm logic product designs.



CD Measurement
Structure: 296 nm x 304 nm
Opaque Via Dot

Resist CD map
CDU= 1.5 nm (3sigma)
CD Range= 3.4 nm

MoSi CD map
CDU= 1.5 nm (3sigma)
CD Range= 3.2 nm

Figure 22. Comparison of across mask global CD uniformity achieved in resist and in final MoSi for a 14 nm via level attenuated PSM mask using resist B2.

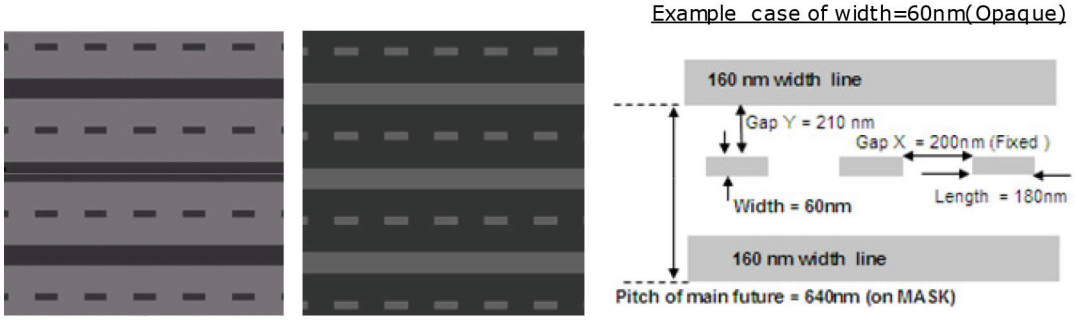


Figure 23. Resolution performance test patterns.

Table 2. Example of manufacturable resolution data for opaque feature (top) and clear features (bottom). Left: Resist A1 on OMOG, Center: Resist A2 on OMOG, Right: Resist B2 on OMOG.

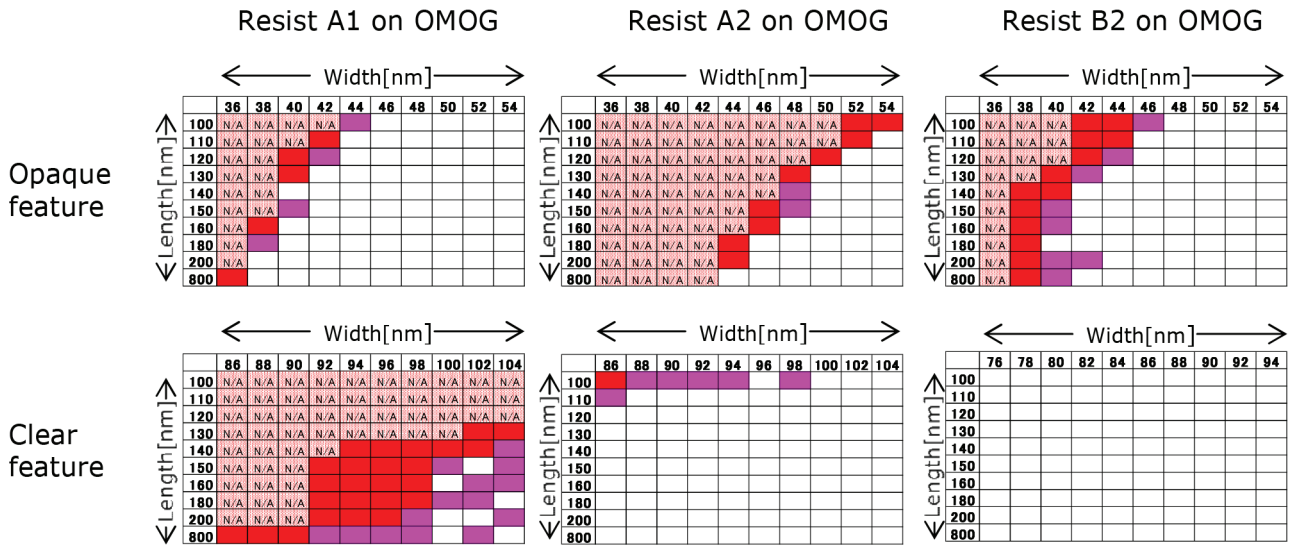
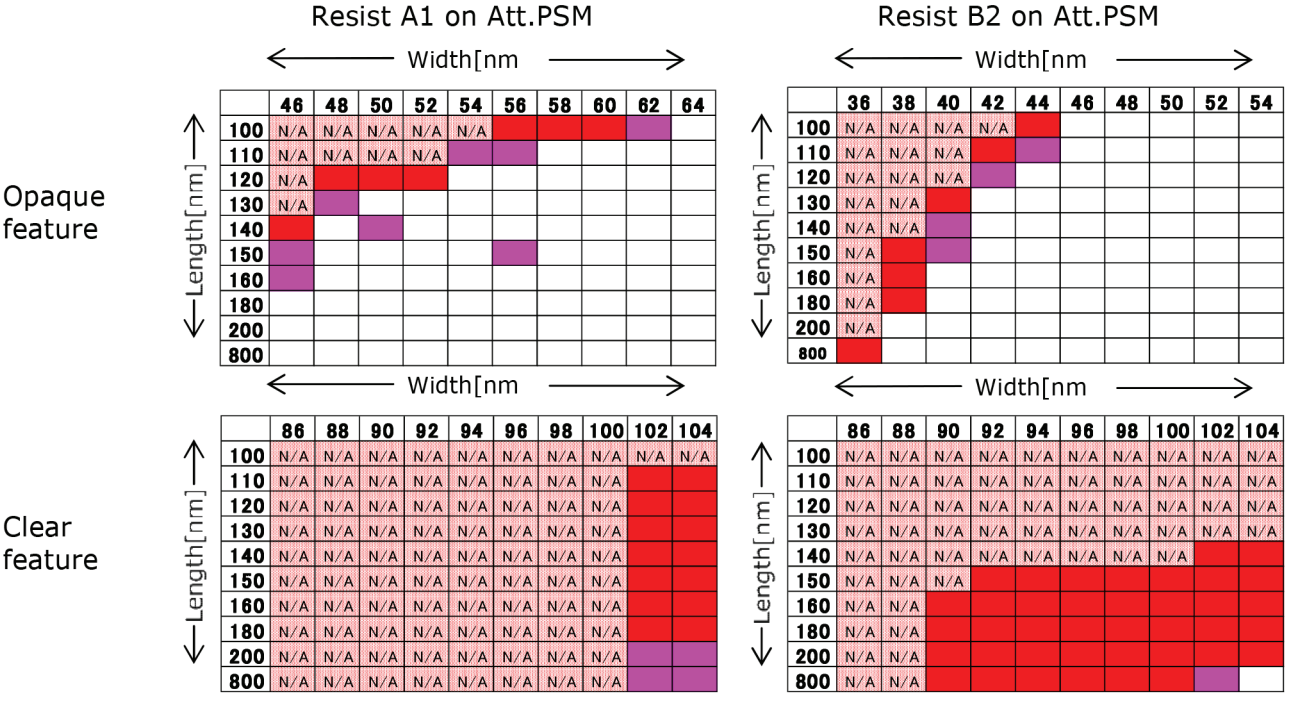


Table 3. Example of manufacturable resolution data for opaque SRAF features (top) and clear features (bottom). Left: Resist A1 on Att. PSM, Right: Resist B2 on Att. PSM.



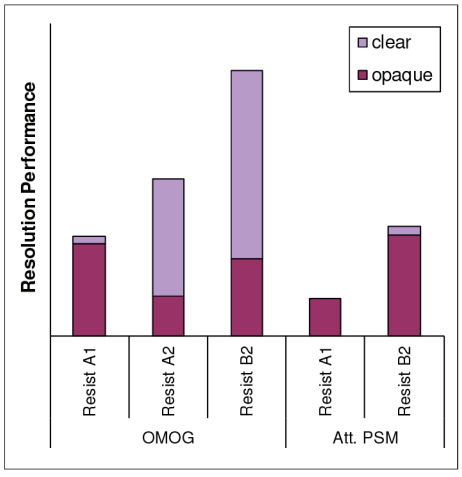


Figure 24. Total resolution performance for NCAR A1, A2, and B2.

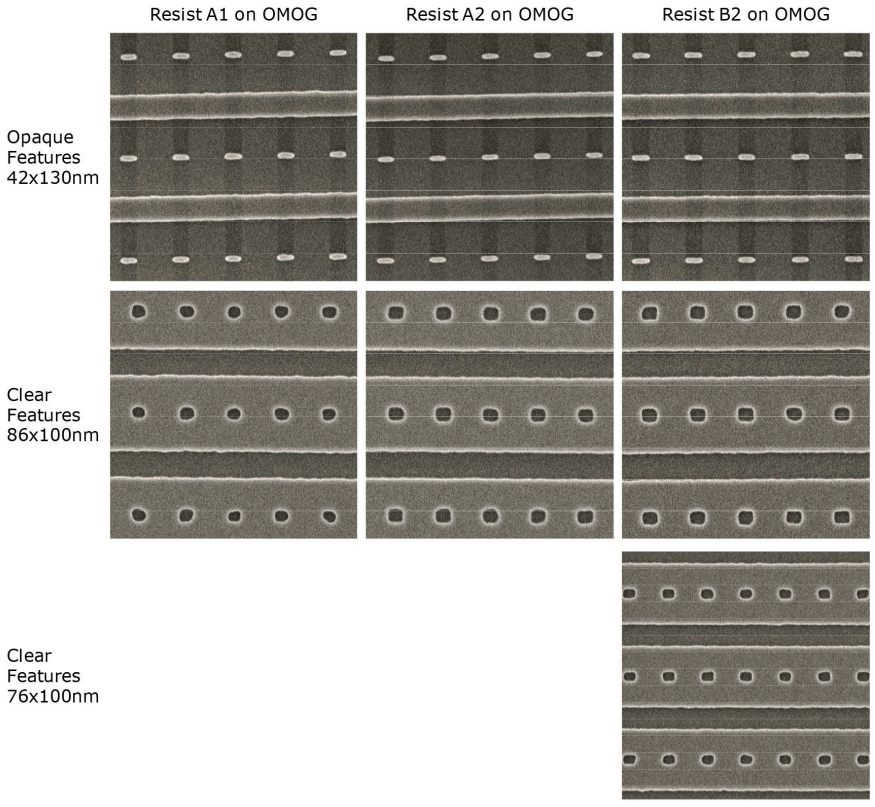


Figure 25. SEM top view SRAF image quality comparison in final MoSi (OMOG type) for resists A1, A2, and B2.

for the top down SEMs were chosen based on the resolution limit of the resists, where opaque SRAF size 44 nm x 120 nm was chosen based on the resolution limit of resist B2 and clear SRAF size 86 nm x100nm was chosen based on the resolution limit of resist A2. As the SEMs indicate the opaque image quality is very similar, but resist A2 shows smaller actual size and worse corner rounding/line end shortening than the other resists. In addition, the image quality of resist B2 clear SRAF features is much better than resist A1.

Figure 26 compares the top down SEM image quality of small opaque and clear SRAFs on attenuated PSM test masks built using resist B2 and resist A1. As indicated in the figure, the 46 nm opaque SRAFs built with resist A1 have more line end shortening and image quality variation than similar opaque SRAFs built with resist B2. In addition, the 104 nm clear SRAF features imaged using resist A1 show more line end shortening and corner rounding than clear SRAF features imaged using resist B2.

These SRAF resolution results are consistent with the benefits of using lower sensitivity polarity switching resist B2 which has better pattern fidelity on opaque features and less scumming in clear features.

7.3 Opaque Dot resolution performance of Attenuated PSM

Figure 27 compares the manufacturable opaque square SRAF dot resolution performance for resists A1 and B2 for attenuated PSM masks. As shown in Figure 28(b), the dots are designed to use the same length and width and have a fixed pitch at 1:4. Square SRAFs of a similar nature are commonly used as part the OPC solution for 14 nm and 10 nm node via level masks. Figure 27 shows that the dot resolution of resist B2 is about 10nm better than resist A1. This result is consistent with the improvement seen in rectangular opaque SRAF resolution for resist B2 on attenuated PSM masks described in the previous section.

8. Summary and Conclusions

A new NCAR e-beam resist has been successfully developed for mask making that uses a novel polarity switching chemistry. Detailed characterization of the resist revealed that it has several key performance advantages compared to the traditional crosslinking NCAR materials that are currently used by the photomask industry. The major advantages of the new polarity switching NCAR are improved minimum feature size, better dry etch resistance, reduced etch loading effect, and improved CD uniformity. In addition, it was verified that the new polarity switching NCAR has acceptable stability with a very reasonable process window as well as acceptable defect density performance. Figure 28 shows examples of the excellent pattern fidelity achieved on a 14 nm logic node attenuated phase shift via level mask. Based on the performance results described in this paper the polarity switching NCAR resist has demonstrated the capability to meet the CD and minimum feature size requirements of 14 nm and 10 nm node logic masks.

9. Acknowledgments

The authors would like to acknowledge the materials, process, metrology, and inspection teams at ShinEtsu, Toppan, and IBM for their tireless efforts to develop this new resist.

10. References

[1] M. Sanchez, L. Sundberg, L. Bozano, R. Sooriyakumaran, D. Sanders, T. Senna, M. Tanabe, T. Komizo, I. Yoshida, and A. Zweber, "Defects on high resolution negative-tone resist: the revenge of the blobs," **Proc. SPIE 8880** (2013).

[2] Zweber, A. E., Faure, T., McGuire, A., Sundberg, L. K., Sooriyakumaran, R., Sanchez, M. I., Bozano, L. D., Senna, T., Fujita, Y., Negishi, Y., Tanabe, M., and Kaneko, T., "Study and comparison of negative tone resists for fabrication of bright field masks for 14 nm node," **Proc. SPIE 8522-27** (2012).

[3] K. Ugajin, M. Saito, M. Suenaga, T. Higaki, H. Nishino, H. Watanabe, and O. Ikenaga, "1 nm of local CD accuracy for 45 nm-node photomask with low sensitivity CAR for e-beam write," **Proc. SPIE Vol. 6607,** 66070A (2007).

[4] A. Saeki, T. Kozawa, and S. Tagawa, "Relationship between resolution, line edge roughness, and sensitivity in chemically amplified resist of post-optical lithography revealed by monte carlo and dissolution simulations," *Appl. Phys. Express 2 Vol. 2(7),* (2009).

[5] A. Zweber, A. Mcguire, M. Hibbs, S. Nash, K. Ballman, T. Faure, J. Rankin, T. Isogawa, T. Senna, Y. Negishi, M. Miller, S. Barai, and D. Dechene, "Two-dimensional mask effects at the 14 nm logic node," **Proc. SPIE 8880** (2013).

[6] International Technology Roadmap for Semiconductors, 2011 ed. www.itrs.net.

[7] H. Gokan, S. Escho, and Y. Ohnishi, "Dry Etch Resistance of Organic Materials," *J. Electrochem. Soc., 130 (1),* 143, (1983).

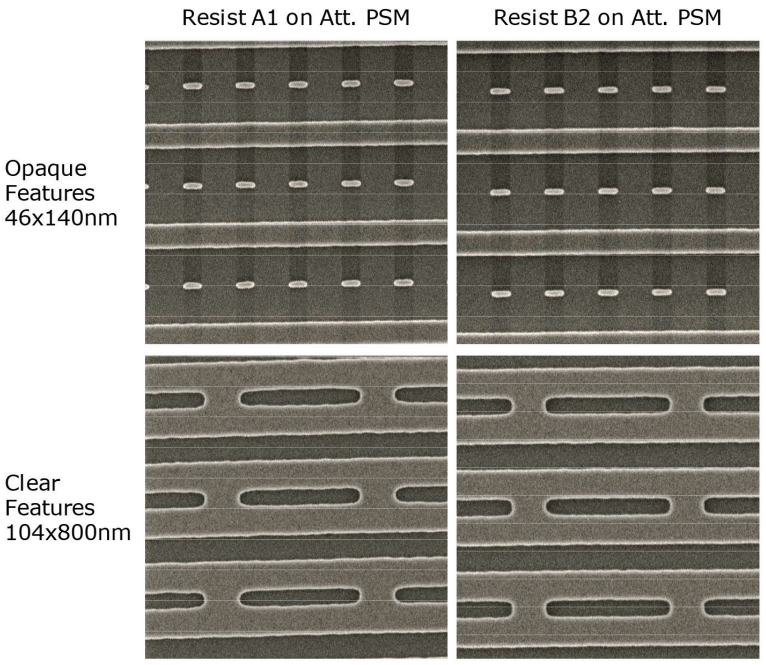
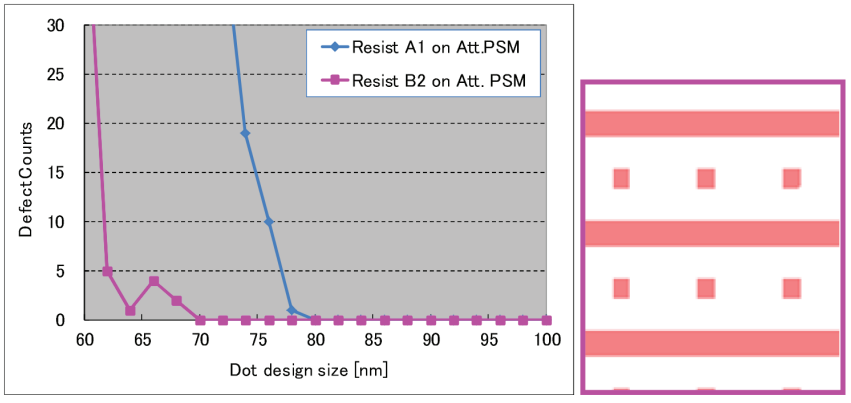
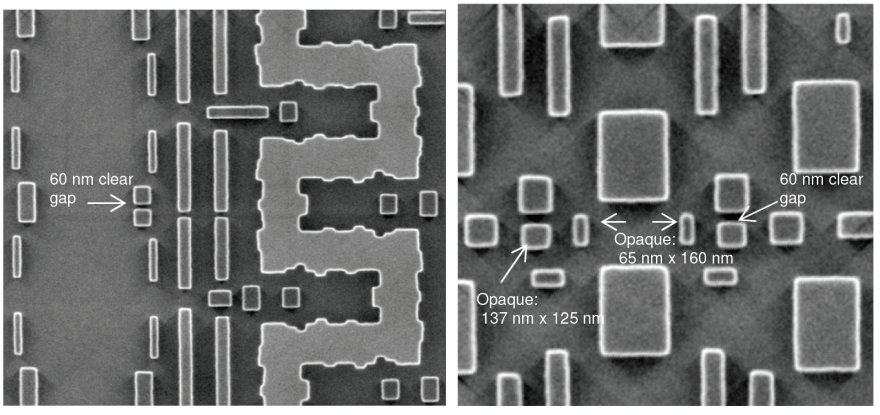


Figure 26. SEM top view SRAF image quality comparison in final MoSi(Att. PSM type)for resist A1 and B2



(a) (b)

Figure 27. (a) Square opaque SRAF dot resolution comparison achieved using resist A1 and resist B2 for attnPSM masks. (b) Square opaque dot test pattern design with 1:4 fixed pitch



(a) (b)

Figure 28. Examples of resist B2 pattern fidelity on 14 nm logic node attenuated PSM via mask: (a) aggressive notch/nub OPC and (b) small opaque SRAFs and clear spaces.

BACUS N • E • W • S

Sponsorship Opportunities

Sign up now for the best sponsorship opportunities

Photomask 2015 —
Contact: Lara Miles, Tel: +1 360 676 3290; laram@spie.org

Advanced Lithography 2015 —
Contact: Lara Miles, Tel: +1 360 676 3290; laram@spie.org

Advertise in the BACUS News!

The BACUS Newsletter is the premier publication serving the photomask industry. For information on how to advertise, contact:

Lara Miles
Tel: +1 360 676 3290
laram@spie.org

BACUS Corporate Members

Acuphase Inc.
American Coating Technologies LLC
AMETEK Precitech, Inc.
Berliner Glas KGaA Herbert Kubatz GmbH & Co.
FUJIFILM Electronic Materials U.S.A., Inc.
Gudeng Precision Industrial Co., Ltd.
Halocarbon Products
HamaTech APE GmbH & Co. KG
Hitachi High Technologies America, Inc.
JEOL USA Inc.
Mentor Graphics Corp.
Molecular Imprints, Inc.
Panavision Federal Systems, LLC
Profilocolore Srl
Raytheon ELCAN Optical Technologies
XYALIS

Industry Briefs

ZEISS AutoAnalysis: New Software Solution

JENA/Germany

The new software solution from Zeiss provides fully automated analysis of ZEISS AIMS aerial images in parallel to the measurements as they are being captured. Manual interaction is no longer required, thus eliminating human error, but still available. Results are automatically entered into customized report layouts. ZEISS AutoAnalysis communicates directly with the ZEISS AIMS tools and has been in use at one customer site for several months. Two more installations will follow in February.

The software was developed by ZEISS in close cooperation with customers. Anthony Garetto, Product Manager at ZEISS says, "For us as a tool supplier, the motivation to enable our customers to shorten turn-around times, improve reliability and save time and manpower was a strong driver to face the challenge of developing a software solution. With our knowledge as the experts in aerial imaging technology and the expertise of our development partners, together we could now release a comprehensive software solution that fits the demands of the mask makers."

SUSS MicroTec and NuFlare Technology Agree on Collaboration

http://goo.gl/FFIDb3 (SUSS MicroTec)

NuFlare Technology, the market leader in electron-beam mask writers and SUSS MicroTec announced a cooperation to combine their expertise in Photomask Equipment and process solutions. NuFlare will install a SUSS MicroTec MaskTrack Pro bake and develop system into their main manufacturing fab, in Yokohama, in early 2015. The MaskTrack Pro system is designed and manufactured to meet the most demanding requirements for masks used in Next Generation Lithography, such as EUVL, 193i extension and Nano-Imprint. Since its release in 2010, more than 30 systems have been shipped to customers worldwide. NuFlare Technology and SUSS MicroTec will jointly work on advanced process solutions, closely integrating the latest NuFlare EB-writer, EBM-9000 and MaskTrack Pro.

"In the semiconductor industry, equipment suppliers are responsible for a smooth and fast start-up of their systems into production," says Yuta Nagai, General Manager of SUSS MicroTec Photomask Equipment. "Our valuable partnership with NuFlare allows both companies to provide solid turn-key equipment and technology solutions to mask makers worldwide."

"Integration between mask writer and develop system is indispensable to accommodate a tighter accuracy request from our high-end customers. I believe the collaboration between SUSS MicroTec and NuFlare will allow us to give them the solution," confirms Fumiaki Shigemitsu, President of NuFlare Technology, Inc.

EUVL – Remaining Challenges and Preview of Topics for the 2015 SPIE EUVL Conference

Vivek Bakshi, EUV Litho, Inc.

With the 2015 SPIE Advanced Lithography (AL) conference around the corner, people have asked what remaining EUVL challenges need to be addressed to ensure it will be ready for mass production later this year or next. The short answer is that we need to see a continued increase in reliable EUV source power in field and address the lack of readiness of EUV mask infrastructure in order for EUVL to be production-worthy in 2016. The long-awaited breakthrough in source power was announced in summer 2014. The availability of 50 W source was a major announcement and morale booster for the EUVL community. One may expect 100 W sources in labs soon and reliable 100 W+ later in 2015.

Delay in the readiness of EUV Mask infrastructure is now the focus of chipmakers. As there is only a single supplier of mask blank deposition tools, progress in defect reduction may come from mask repairs and by avoiding the addition of defects during manufacturing with the help of pellicles and mask cleans. Lack of readiness of actinic mask inspection tools remains a big gap. In the near term, EUVL extension may come via multiple patterning and not via high NA options (which comes combined with a need to go to larger 9"masks).

Join the premier professional organization for mask makers and mask users!

About the BACUS Group

Founded in 1980 by a group of chrome blank users wanting a single voice to interact with suppliers, BACUS has grown to become the largest and most widely known forum for the exchange of technical information of interest to photomask and reticle makers. BACUS joined SPIE in January of 1991 to expand the exchange of information with mask makers around the world.

The group sponsors an informative monthly meeting and newsletter, BACUS News. The BACUS annual Photomask Technology Symposium covers photomask technology, photomask processes, lithography, materials and resists, phase shift masks, inspection and repair, metrology, and quality and manufacturing management.

Individual Membership Benefits include:

- Subscription to BACUS News (monthly)
- Eligibility to hold office on BACUS Steering Committee

www.spie.org/bacushome

Corporate Membership Benefits include:

- 3-10 Voting Members in the SPIE General Membership, depending on tier level
- Subscription to BACUS News (monthly)
- One online SPIE Journal Subscription
- Listed as a Corporate Member in the BACUS Monthly Newsletter

www.spie.org/bacushome

Calendar

2015

SPIE Photomask Technology
Co-located with
SPIE Scanning Microscopies
29 September-1 October 2015
Monterey Marriott and
Monterey Conference Center
Monterey, California, USA

SPIE Scanning Microscopies
Co-located with
SPIE Photomask Technology
29 September-1 October 2015
Monterey Marriott and
Monterey Conference Center
Monterey, California, USA

SPIE is the international society for optics and photonics, a not-for-profit organization founded in 1955 to advance light-based technologies. The Society serves nearly 225,000 constituents from approximately 150 countries, offering conferences, continuing education, books, journals, and a digital library in support of interdisciplinary information exchange, professional growth, and patent precedent. SPIE provided over $3.4 million in support of education and outreach programs in 2014.

SPIE.
International Headquarters
P.O. Box 10, Bellingham, WA 98227-0010 USA
Tel: +1 360 676 3290
Fax: +1 360 647 1445
help@spie.org • www.SPIE.org

Shipping Address
1000 20th St., Bellingham, WA 98225-6705 USA

Managed by SPIE Europe
2 Alexandra Gate, Ffordd Pengam, Cardiff,
CF24 2SA, UK
Tel: +44 29 2089 4747
Fax: +44 29 2089 4750
spieeurope@spieeurope.org • www.spieeurope.org

You are invited to submit events of interest for this calendar. Please send to lindad@spie.org; alternatively, email or fax to SPIE.